AJNR

Curved Planar Reformatted CT Angiography: Usefulness for the Evaluation of Aneurysms at the Carotid Siphon

Takashi Ochi, Kenji Shimizu, Yoshifumi Yasuhara, Toshirou Shigesawa, Teruhito Mochizuki and Junpei Ikezoe

AJNR Am J Neuroradiol 1999, 20 (6) 1025-1030
http://www.ajnr.org/content/20/6/1025

AJNR Am J Neuroradiol 20:1025–1030, June/July 1999

Curved Planar Reformatted CT Angiography: Usefulness for the Evaluation of Aneurysms at the Carotid Siphon

Takashi Ochi, Kenji Shimizu, Yoshifumi Yasuhara, Toshirou Shigesawa, Teruhito Mochizuki, and Junpei Ikezoe

BACKGROUND AND PURPOSE: **Three-dimensional CT angiography uses the data obtained on a contrast-enhanced CT brain scan to generate 3D images of the intracranial vasculature. We describe the methodology of curved planar reformatting (CPR) for CT angiography and characterize its usefulness in the evaluation of aneurysms at the carotid siphon, comparing it with the shaded surface display technique (SSD).**

METHODS: **Eighty-seven patients with suspected intracranial aneurysms at CT angiography were examined by conventional cerebral angiography, and the patients with aneurysm(s) at the carotid siphon were selected for study. For these patients, the visibility of the neck and fundus of the aneurysms on CT angiograms was compared for those obtained with SSD and those with CPR, and observer reproducibility was evaluated with the κ statistic.**

RESULTS: **Eighteen patients were confirmed to have an aneurysm at the carotid siphon on conventional angiograms. Seventeen aneurysms were depicted at CT angiography with SSD; 18 aneurysms with CPR. The number of visible aneurysmal necks and fundi was nine and 12, respectively, with SSD; 18 and 18, respectively, with CPR.**

CONCLUSION: **CPR allows better demonstration of the body and neck of an aneurysm at the carotid siphon, which has a tortuous course and is surrounded by complex bony structures. CPR may be a useful adjunct for the evaluation of aneurysms in this region.**

CT angiography, which is made possible by contrast-enhanced fast sequential or spiral CT scanning and computerized 3D rendering techniques, has been introduced as a minimally invasive technique for vascular imaging (1–9). CT angiography can provide unique information, compared with that available from conventional angiography. Currently, the CT data can be processed to produce vascular images in three different ways: shaded surface display (SSD) (1, 3–7, 9), maximum intensity projection (2–4, 6, 8, 9), and multi- or curved planar reformatting (CPR) (4, 10, 11). The SSD technique has the advantage of providing excellent 3D visualization of a lesion of the cerebral vascular and its relation to surrounding vascular and skeletal structures (12–15). Three-dimensional CT angiography with SSD has been proved efficacious in the evaluation and surgical planning of intracranial aneurysms, especially in complex aneurysms of the circle of Willis (16–22).

Received August 21, 1998; accepted after revision February 2, 1999.

From the Department of Radiology, Ehime University School of Medicine, Shitsukawa, Shigenobu, Ehime 791-0295, Japan.

Address reprint requests to Kenji Shimizu, MD, PhD.

The SSD technique, however, has some limitations in depicting aneurysms at the carotid siphon, which has a tortuous course and is surrounded by complex bony structures. Threshold-based surface rendering of the SSD technique has difficulty in separating contrast-enhanced vessels from the skull base bone, owing to partial volume effects. With SSD, highly attenuating, overlapping skeletal structures can mask target anatomy, and neighboring bony structures, such as the anterior clinoid process, may limit the perspective. The tortuous course of the carotid siphon may overlap an aneurysm, possibly resulting in failure to see the aneurysmal neck and body with SSD. Thus, vascular abnormalities within this region cannot be evaluated accurately only with this technique.

For tortuous vessels, flexible multiplanar reformatting along the course of the target artery can be performed by using an axial image as a reference to define the course of the desired reformation. This technique, known as CPR, has been shown to be useful in displaying both renal arteries and the abdominal aorta in a single plane (4). The CPR technique has also successfully demonstrated the course of the ureter (11). Therefore, CPR may have potential advantages for evaluating aneurysms at the carotid siphon. We describe the CPR technique and report our initial experience in its application to

aneurysms at the carotid siphon. We also compare the CPR findings with those of SSD and discuss the role of this technique in the evaluation of aneurysms at the carotid siphon.

Methods

CPR Technique

The procedure of the CPR technique is as follows. First, axial sections, including a volume of interest, are stacked to generate an imaging volume. Then, a reformatting algorithm is applied to the arbitrarily rotated imaging volume. For a composite sagittal CPR image, a coronal section is selected as the reference plane. The viewer pages through a series of contiguous reference images from a volumetric data set. On each image within these contiguous reference images, the course of the target vessel is traced by a series of mouse clicks. This procedure continues until the entire course of the target vessel within the volume of interest has been traced. Then, along the defined curved line, a single-voxel-thick plane, orthogonal to the reference plane, is extruded through the entire data set. Finally, the resultant ''curved plane'' is flattened and displayed as a 2D, composite sagittal image representing the target vessel. In practice, the stacked CT scans have been rotated around the rostral-caudal axis to place the long axis of an aneurysm on the sagittal plane before CPR is applied.

CT Examination

CT angiographic studies were performed on a commercially available scanner (Xvigor, Toshiba Medical Systems, Tokyo), according to the following protocol. First, a lateral scanogram was obtained to define landmarks for the initiation and termination points of the CT angiographic study. After the selection of a starting point at a level approximately 10 mm below the floor of the sella turcica, 2 mL/kg of nonionic iodinated contrast material (iopamidol, 300 mg I/mL) was delivered through a 20-gauge antecubital intravenous catheter by using a power injector at the rate of 2 mL/s. Twenty-five seconds after the initiation of contrast injection, helical CT scanning was started, with the scan plane parallel to the supraorbital-meatal line. The CT scan acquisition was performed with 1-mm collimation, 1-mm/s table feed, and 1:1 pitch, covering at least 45 mm in the rostral-caudal direction. The scanning parameters were 135 kV, 150 mA, and a 30-cm field of view.

After scanning was completed, images of 1-mm-thick sections were reconstructed every 0.5 mm using a 180° linear interpolation algorithm with a 512 × 512 matrix, resulting in 100 images of 1-mm-thick sections, each of which overlapped 0.5 mm with its adjacent section. These source axial images were transferred to a dedicated workstation (Xtension, Toshiba Medical Systems, Tokyo) to create a 3D matrix of image data. Then, the 3D CT angiograms were reconstructed in color-coded SSD: the vasculature showing 100 to 280 HU was orange and the calcification and bone showing over 280 HU were white. Finally, CPR was applied to produce a composite sagittal reformatted image along the course of the carotid siphon. The average processing time after the axial images were reconstructed and transferred was 40 and 30 minutes for SSD and CPR, respectively.

Patient Selection and Image Interpretation

From June 1995 through February 1998, 205 patients (107 men and 98 women, ranging in age from 8 to 76 years) referred for the diagnosis and preoperative evaluation of suspected vascular abnormalities underwent 3D CT angiography at our institution. Because of aneurysms suspected on the basis of findings on source axial images and their SSD reconstructions, 87 patients (58 women and 29 men, ranging in age from 26 to 76 years) were further examined by conventional cerebral angiography. Two experienced neuroradiologists independently reviewed findings of conventional angiography in these 87 patients; then, 18 patients (15 women and three men, ranging in age from 26 to 76 years; mean age, 60 years) with aneurysm(s) at the carotid siphon were selected by consensus for subsequent evaluation.

The 3D CT angiograms acquired with SSD and CPR were separately and independently interpreted by three other neuroradiologists, who had no knowledge of the findings on conventional angiograms. Although these reviewers had not worked with the SSD and CPR techniques, they could differentiate the images produced by the two methods. When an aneurysm was identified, the visibility of the neck and fundus was subjectively evaluated on the SSD and CPR images. A neck was considered to be present if an aneurysm narrowed to 80% or less of its maximum transverse diameter at the site of attachment to its vessel of origin. If a circumferential view of an aneurysm could be achieved, a fundus was considered to be present. Observers also looked for mural calcification and intraaneurysmal thrombus. The size of the aneurysm was measured directly on the source axial CT scans.

Statistical Analysis

Interobserver variability among the three reviewers with regard to the visibility of the neck and fundus was analyzed by using the κ statistic (23). The level of agreement was defined as follows: κ values of less than 0 indicated no agreement; κ values of 0.00 to 0.40 indicated poor agreement; κ values of 0.41 to 0.75 represented good agreement; and κ values of 0.76 to 1.00 represented excellent agreement.

Results

The clinical applications and findings on conventional angiography and/or surgery in this series of 18 patients are summarized in Table 1. Each patient had one aneurysm; thus, 18 aneurysms with diameters ranging from 3 to 25 mm were included in the study. Of these, 17 aneurysms could be identified with SSD and 18 aneurysms with CPR by the three independent observers. An infraclinoid, small aneurysm of the left internal carotid artery–ophthalmic artery could not be detected with SSD (Fig 1). Assessment of the visibility of the neck and fundus of the aneurysms is summarized in Table 2. Fewer necks and fundi were identified with the SSD technique. Interobserver variability for the two reviewers (1 vs 2, 1 vs 3, 2 vs 3) showed excellent agreement for ability to identify the neck and fundus with both techniques (Table 3). Representative cases exemplifying the performance of the SSD and CPR techniques are presented below.

Representative Cases

Case 1: A 58-year-old woman with a possible aneurysm on an MR angiogram obtained at another institution was referred for further evaluation. Conventional angiography revealed an aneurysm measuring approximately 3 mm in diameter at the C3 portion of the right internal carotid artery (Fig 2A). The aneurysm was surrounded by bony structures, with approximation of its dome to the sella tubercle. Owing to the partial volume effect of the skull

Table 1: Summary of 18 patients with an aneurysm at the carotid siphon

Patient	Age (y)/Sex	Clinical Presentation	Site of Aneurysm	Size of Artery (mm)
1	58/F	Gait disturbance	RICA-Oph	3
2	63/M	Dizziness	LICA-Oph	4
3	41/F	Headache	LICA-Oph	3
4	34/M	Seizure	LICA-Oph	3
5	62/F	Headache	LICA-Oph	3
6	38/F	R hemiparesis	LICA-PComA	3
7	67/F	Headache	LICA-Oph	5
8	70/F	Headache	LICA-Oph	3
9	69/F	Dysphasia	RICA-PComA	7
10	76/F	Seizure	LICA-PComA	3
11	71/F	R oculomotor palsy	RICA-Oph	25
12	74/F	Diplopia	LICA-PComA	7
13	60/F	R hemiparesis	RICA-PComA	15
14	76/F	Seizure	RICA-PComA	7
15	74/M	Disorientation	LICA-PComA	3
16	26/F	R trigeminal neuralgia	LICA-Oph	4
17	62/F	SAH	LICA-PComA	8
18	58/F	Vertigo	LICA-Oph	3

Note.—SAH indicates subarachnoid hemorrhage; ICA, internal carotid artery; Oph, ophthalmic artery; PComA, posterior communicating artery.

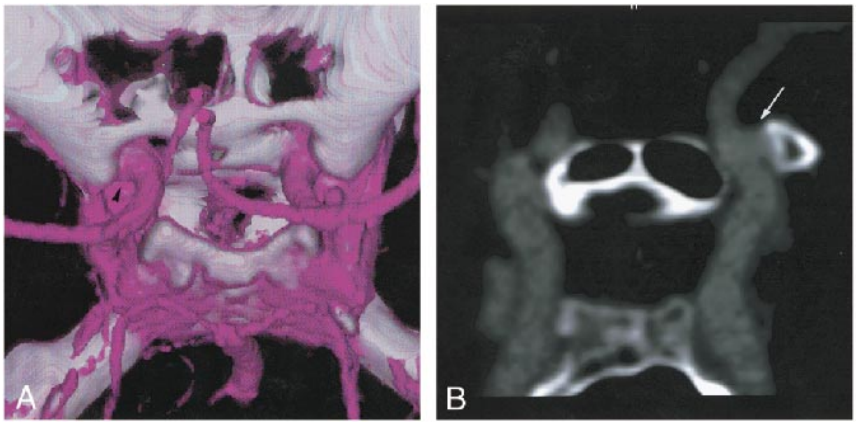

FIG 1. Patient with an infraclinoid, small aneurysm of the left internal carotid artery–ophthalmic artery.

A, 3D CT angiogram with SSD (superoposterior view) shows a slight laterally bulging contour (*arrowhead*); however, a significant saccular component cannot be identified.

B, Composite sagittal CPR image clearly shows a small aneurysm (*arrow*) adherent to the anterior clinoid process.

Table 2: Number of visible aneurysmal necks and fundi

	SSD (n = 17)		CPR (n = 18)	
Observer	Neck	Fundus	Neck	Fundus
1	9	12	18	18
2	8	11	18	17
3	8	11	18	17

Note.—SSD indicates shaded surface display; CPR, curved planar reformatting.

Table 3: κ values for interobserver variability

	SSD (n = 17)		CPR (n = 18)	
Observer	Neck	Fundus	Neck	Fundus
1 vs 2	0.88	0.87	1.00	0.95
1 vs 3	0.88	0.87	1.00	0.95
2 vs 3	1.00	1.00	1.00	1.00

Note.—SSD indicates shaded surface display; CPR, curved planar reformatting.

base bone, clear-cut surfaces were difficult to define by the threshold-based SSD rendering method. As a result, the fundus of the aneurysm could not be appreciated correctly with SSD (Fig 2B). In contrast, the composite sagittal CPR image clearly showed the fundus and neck of the aneurysm and its projection direction relative to the parent artery (Fig 2C).

Case 11: A 71-year-old woman with a giant aneurysm of the right internal carotid artery visible on a contrast-enhanced CT scan obtained at another institution was referred for further evaluation. Conventional angiography revealed an aneurysm measuring approximately 25 mm in diameter at the C3 portion of the right internal carotid artery (Fig 3A). The neck of the aneurysm in relation to the parent artery could not be appreciated by conventional angiography owing to the limited number of views available. Although SSD showed a circumferential view of the aneurysm and its relation to the cranial base, the giant fundus prevented SSD from depict-

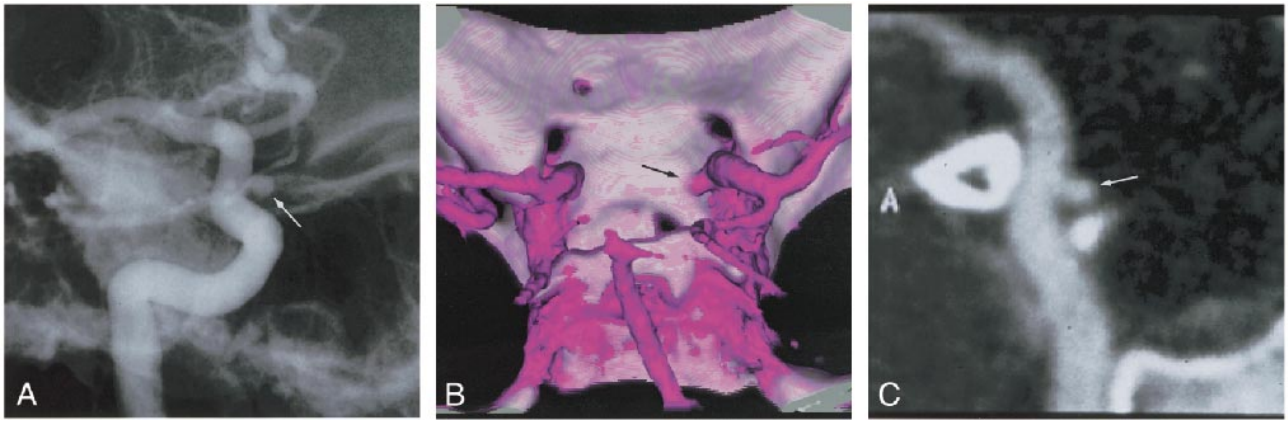

FIG 2. Case 1: Patient with an aneurysm of the right internal carotid artery–ophthalmic artery.
A, Right carotid angiogram (left anterior oblique view) shows an aneurysm of the internal carotid artery–ophthalmic artery (*arrow*).
B, 3D CT angiogram with SSD (superoposterior view) shows an aneurysm (*arrow*). The fundus cannot be correctly rendered with the SSD technique owing to partial volume effects of the skull base bone.
C, Composite sagittal CPR image clearly shows the fundus and neck of the aneurysm (*arrow*).

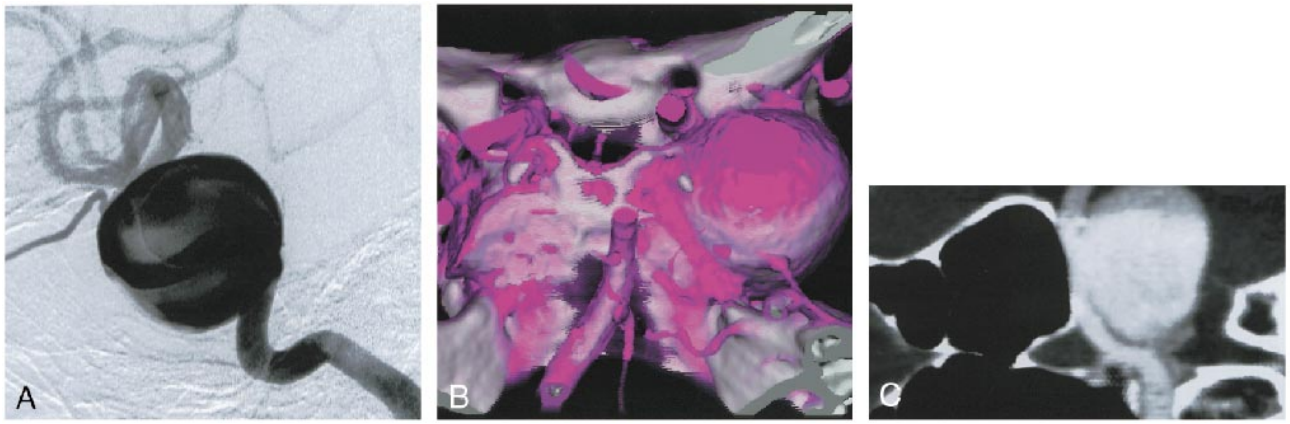

FIG 3. Case 11: Patient with an aneurysm of the right internal carotid artery–ophthalmic artery.
A, Right carotid angiogram (left lateral view) shows a giant aneurysm.
B, 3D CT angiogram with SSD (superoposterior view) shows an aneurysm. The neck cannot be identified with the SSD technique owing to the giant overlapping fundus.
C, Composite sagittal CPR image clearly shows the neck of the aneurysm with the associated vessel of origin.

ing the neck (Fig 3B). On the other hand, the composite sagittal CPR image clearly showed a broad but well-defined aneurysmal neck with the associated vessel of origin (Fig 3C).

Case 13: A 60-year-old woman had an aneurysm of the right internal carotid artery–posterior communicating artery. Conventional angiography revealed an aneurysm measuring approximately 15 mm in diameter at the C2 portion of the right internal carotid artery (Fig 4A). Calcification could not be seen at conventional angiography; and, although calcification was observed with SSD, the mural calcium could not be precisely evaluated owing to the limitation of the surface rendering technique (Fig 4B). The composite sagittal CPR image showed a well-defined aneurysmal neck emanating straight from the parent artery, as well as calcification in the wall of the aneurysm and parent artery (Fig 4C).

Discussion

Three-dimensional CT angiography is a combined technology of contrast-enhanced fast sequential or spiral CT scanning and computerized 3D reconstruction. Three-dimensional renderings remove the constraints of transverse tomographic imaging, allowing anatomy to be viewed from multiple angles. Therefore, they provide an exquisite view of complex 3D relationships of cerebral vasculature (12–15), especially in the circle of Willis (16–22). An important role of 3D CT angiography is as an adjunct to conventional angiography, because it can provide surgically important information about the shape and direction of an aneurysm and its relation to surrounding arteries and neighboring bone structures (16–20).

In this study, the SSD technique failed to show an infraclinoid, small aneurysm (Fig 1A), which

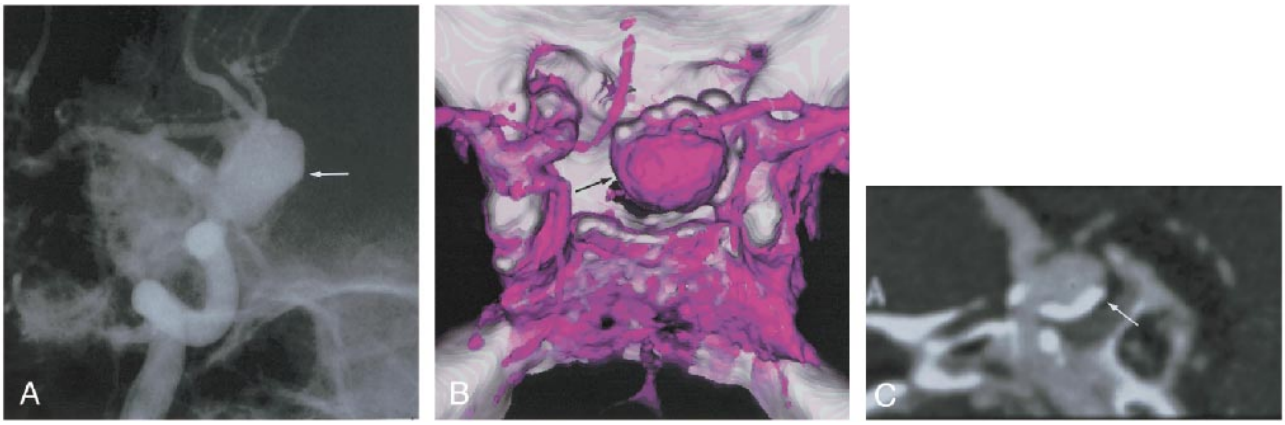

FIG 4. Case 13: Patient with an aneurysm of the internal carotid artery–posterior communicating artery.
A, Right carotid angiogram (left anterior oblique view) shows an aneurysm (*arrow*).
B, 3D CT angiogram with SSD (superior view) shows an aneurysm (*arrow*). Mural calcium cannot be well appreciated.
C, Composite sagittal CPR image clearly shows calcification in the wall of the aneurysm (*arrow*) and parent artery.

was well demonstrated with CPR (Fig 1B). This result represents a limitation of 3D CT angiography with SSD reconstruction as a screening tool, especially for small aneurysms. Because the CPR technique is more interactive, additional information can be gained, even in relation to small aneurysms.

The SSD technique used threshold-based processing, in which contiguous voxels at the boundary of a predefined threshold range are modeled as surfaces by the computer. With this processing, the surface of an aneurysm adjacent to bony structures may not be well demonstrated against the bony background, owing to partial volume effects of the skull base bone. In our series, the fundus of one aneurysm could not be appreciated correctly with SSD because of its adherence to the sella tubercle (Fig 2B). Furthermore, threshold selection profoundly affects the appearance of an aneurysm and parent artery. Improper thresholding can markedly alter the appearance of the vessels and potentially result in elimination of vascular branches or aneurysms (1, 4–6).

The SSD technique presents difficulty with delineating an aneurysm when it is overlapped by dense or bony structures that cannot be eliminated with postprocessing. Highly attenuating bone structures limit the perspective available to display target anatomy with SSD. In our study, a small aneurysm located beneath the anterior clinoid process was not apparent with the SSD technique. To evaluate these aneurysms, the overlying adjacent bony structures that hamper evaluation of these aneurysms should be removed by manual editing. However, elimination of osseous structures can be particularly challenging. The SSD technique may also introduce false-positive results by causing the bending of an artery to be misinterpreted as an aneurysm. Large or giant aneurysms, overlapping the parent artery, make it difficult to visualize the neck of an aneurysm with SSD (Fig 3B).

In this study, calcification at the inner surface of the aneurysm could not be precisely evaluated with SSD owing to the limitation of the surface rendering technique (Fig 4B). For partially thrombosed aneurysms, the actively filling versus thrombosed portions could not be envisioned with SSD. To demonstrate mural calcification or thrombus as well as the actively filling portions of an aneurysm on the same image, a slice should be cut through the center of the aneurysm to display structures inside or behind the surface.

Another rendering technique is multiplanar reformation, in which coronal, sagittal, or oblique single-voxel-thick planes are created from the stacked transverse sections. They are excellent for displaying anatomic relationships that vary along any single arbitrary direction. Because arteries are not constrained to a specific plane, it is rare to visualize an artery along its entire course on a single reformatted section. Tortuous vessels, such as the carotid siphon, will be separated into fragments on a single plane by multiplanar reformations. In contrast, the CPR technique can be helpful for displaying tortuous vessels that cannot be visualized completely throughout their entire course on a flat planar section. The course of the desired reformation is prescribed from a curve drawn on each reference image, which is then extended through the entire data set. The resultant curved plane is flattened and displayed as a 2D image.

The CPR technique is not threshold-dependent and does not suffer from the limitations caused by partial volume effects. Therefore, the fundus and neck of an aneurysm in contact with the skull base bone can be well appreciated on a CPR image (Fig 2C). This technique can also obviate the limitation of view angle caused by bony structures, including the anterior clinoid process. CPR preserves all the relative attenuation information of contrast medium, intraluminal thrombus, mural calcification, and bone. Intravascular contrast material in an aneu-

rysm and calcified atheroma or high-attenuation blood clot of the aneurysm can be discriminated with CPR.

The planar nature of the CPR technique enables evaluation of the neck of an aneurysm beneath overlapping tortuous vessels. For large or giant aneurysms, the neck can be delineated by the CPR technique even with a large overlapping fundus (Fig 3C). The composite CPR image can cut through the aneurysm and reveal its inner surface, allowing display of the mural calcification and/or intraluminal thrombus and its relation to the aneurysmal neck (Fig 4C).

The ability of the CPR technique over SSD to depict the aneurysmal neck and the most proximal projection of the aneurysm relative to the parent artery is advantageous for evaluating the clippability of an aneurysm (16–20).

The CPR technique does, however, have some limitations. With CPR, distances are referenced to the curve and not to the Cartesian coordinate system of other planar images. Spatial relationships and the projection direction of an aneurysm to all other structures cannot be appreciated from a CPR image. Distances should not be measured from CPR images. Therefore, when assessing the relative position of structures, CPR images must be interpreted in association with axial sections and other 3D-rendered images.

Another disadvantage is that the CPR technique is highly operator-dependent and can be time-consuming. Displays do not incorporate information from adjoining voxels and thus inaccurate plane selection can falsely simulate lesions that are not present or can exclude true lesions from the rendering. Therefore, precise evaluation of the target vessel, which is separated into fragments on each reference image, is always required to exclude inaccuracies. This manual technique requires specialized training of an operator who has good knowledge of cerebral vascular anatomy.

Conclusion

CPR is a planar reformation along a curve to create a composite reformatted plane on which a tortuous vessel is readily appreciated. It enables good demonstration of an aneurysm's body and neck as well as its relation to the vessel of origin. Although the CPR technique has some limitations, the reformatted images generated by this technique can provide unique information not readily available from other imaging methods. Therefore, CPR may be a useful adjunct for the evaluation of aneurysms at the carotid siphon.

References

1. Schwartz RB, Jones KM, Chernoff DM, et al. **Common carotid artery bifurcation: evaluation with spiral CT.** *Radiology* 1992; 185:513–519
2. Napel S, Marks MP, Rubin GD, et al. **CT angiography with spiral CT and maximum intensity projection.** *Radiology* 1992;185: 607–610
3. Rubin GD, Dake MD, Napel S, McDonnell CH, Jeffrey RB. **Three-dimensional spiral CT angiography of the abdomen: initial clinical experience.** *Radiology* 1993;186:147–152
4. Galanski M, Prokop M, Chavan A, et al. **Renal arterial stenoses: spiral CT angiography.** *Radiology* 1993;189:185–192
5. Dillon EH, van Leeuwen MS, Fernandez MA, et al. **CT angiography: application to the evaluation of carotid artery stenosis.** *Radiology* 1993;189:211–219
6. Rubin GD, Dake MD, Napel S, et al. **Spiral CT of renal artery stenosis: comparison of three-dimensional rendering techniques.** *Radiology* 1994;190:181–189
7. Dillon EH, van Leeuwen MS, Fernandez MA, Mali WPTM. **Spiral CT angiography.** *AJR Am J Roentgenol* 1993;160:1273–1278
8. Marks MP, Napel S, Jordan JE, Enzmann DR. **Diagnosis of carotid artery disease: preliminary experience with maximum-intensity-projection spiral CT angiography.** *AJR Am J Roentgenol* 1993;160:1267–1271
9. Zeman RK, Davros WJ, Berman P, et al. **Three-dimensional models of the abdominal vasculature based on helical CT: usefulness in patients with pancreatic neoplasms.** *AJR Am J Roentgenol* 1994;162:1425–1429
10. Fishman EK, Wyatt SH, Ney DR, Kuhlman JE, Siegelman SS. **Spiral CT of the pancreas with multiplanar display.** *AJR Am J Roentgenol* 1992;159:1209–1215
11. Sommer FG, Jeffrey RB, Rubin GD. **Detection of ureteral calculi in patients with suspected renal colic: value of reformatted noncontrast helical CT.** *AJR Am J Roentgenol* 1995;165:509–513
12. Aoki S, Sasaki Y, Machida T, et al. **Cerebral aneurysms: detection and delineation using 3-D-CT angiography.** *AJNR Am J Neuroradiol* 1992;13:1115–1120
13. Alberico RA, Patel M, Casey S, et al. **Evaluation of the circle of Willis with three-dimensional CT angiography in patients with suspected intracranial aneurysms.** *AJNR Am J Neuroradiol* 1995;16:1571–1578
14. Hope JKA, Wilson JL, Thomson FJ. **Three-dimensional CT angiography in the detection and characterization of intracranial berry aneurysms.** *AJNR Am J Neuroradiol* 1996;17:439–445
15. Ogawa T, Okudera T, Noguchi K, et al. **Cerebral aneurysms: evaluation with three-dimensional CT angiography.** *AJNR Am J Neuroradiol* 1996;17:447–454
16. Harbaugh RE, Schlusselberg DS, Jeffery R, et al. **Three-dimensional computerized tomography angiography in the diagnosis of cerebrovascular disease.** *J Neurosurg* 1992;76:408–414
17. Dorsch NWC, Young N, Kingston RJ, Compton JS. **Early experience with spiral CT in the diagnosis of intracranial aneurysms.** *Neurosurgery* 1995;36:230–238
18. Harbaugh RE, Schlusselberg DS, Jeffery R, et al. **Three-dimensional computed tomographic angiography in the preoperative evaluation of cerebrovascular lesions.** *Neurosurgery* 1995;36: 320–327
19. Tampieri D, Leblanc R, Oleszek J, et al. **Three-dimensional computed tomographic angiography of cerebral aneurysms.** *Neurosurgery* 1995;36:749–755
20. Zouaoui A, Sahel M, Marro B, et al. **Three-dimensional computed tomographic angiography in detection of cerebral aneurysms in acute subarachnoid hemorrhage.** *Neurosurgery* 1997;41:125–130
21. Vieco PT, Shuman WP, Alsofrom GF, Gross CE. **Detection of circle of Willis aneurysms in patients with acute subarachnoid hemorrhage: a comparison of CT angiography and digital subtraction angiography.** *AJR Am J Roentgenol* 1995;165:425–430
22. Rieger J, Hosten N, Neumann K, et al. **Initial clinical experience with spiral CT and 3D arterial reconstruction in intracranial aneurysms and arteriovenous malformations.** *Neuroradiology* 1996;38:245–251
23. Davies M, Fleiss JL. **Measuring agreement for multinominal data.** *Biometrics* 1982;38:1047–1051